Absorption Spectroscopy of the Continuous Transition from Low to High Electron Density in a Single Modulation-Doped InGaAs Quantum Well

I. Bar Joseph, J. M. Kuo, C. Klingshirn, G. Livescu, T. Y. Chang, D. A. B. Miller, and D. S. Chemla
AT&T Bell Laboratories, Holmdel, New Jersey 07733
(Received 23 April 1987)

We perform differential absorption spectroscopy of a single modulation-doped InGaAs quantum well as its electron density is varied continuously from full ($N \approx 8\times10^{11}$ cm^{-2}) to empty ($N \approx 0$) by a gate electrode, allowing direct measurement of the density-dependent changes of transition energies and strengths. We observe a progressive quenching of the optical transition at the first subband and red shifts and broadening at higher subbands. We show that the dominant mechanisms are phase-space filling and the quantum-confined Stark effect. This technique also allows direct *in situ* measurements of the density and temperature of the 2D electron gas in such field-effect–transistor structures.

PACS numbers: 78.20.Dj, 73.20.Dx

Recently quantum size effects in ultrathin (≈ 100 Å) semiconductor quantum wells (QW's) have attracted much interest both for fundamental physics and for their potential applications to electronics and optoelectronics.[1] Undoped QW's exhibit enhanced excitonic behavior of particular interest for optics[2] whereas modulation-doped (MD) QW's show very attractive electronic transport properties.[3] The absorption spectra of undoped III-V semiconductor QW's show well-resolved exciton resonances at the onset of each intersubband transition. These resonances remain clearly visible even at room temperature.[2] In MD QW's, the occupation of the conduction (valence) subbands by the two-dimensional electron (hole) gas produces a blue shift of the absorption edge similar to the Burstein-Moss effects seen in bulk semiconductors. The intrinsic luminescence still occurs at the fundamental gap.[4,5] Recent investigations have revealed that electron-hole correlation singularities appear near the Fermi energy E_F and that even at large doping densities exciton resonances persist at the onset of the high-energy intersubband transitions ($n_z=2$).[6] The presence of carriers in the QW's also produces band-gap renormalization (BGR) through correlation and exchange.[7]

Up to now comparisons of the electronic structures of the two types of QW's were made on different samples, with all the unavoidable fluctuations of parameters this implies. There have been some attempts to change the concentration of carriers in MD QW's by photoexcitation.[8] Such simultaneous injection of both electrons and holes into the QW has, among other things, very different electrostatic consequences from addition of electrons alone. Furthermore, those investigations performed by photoluminescence are limited to the energies close to the first transition, while those using excitation spectroscopy rely on a two-step mechanism and therefore cannot be a basis for reliable quantitative line-shape analysis. Absorption spectroscopy, on the other hand, gives direct quantitative information on the intrinsic optical properties, and is therefore preferred whenever possible.

In this Letter we present the first investigation of the changes in the intrinsic absorption which occur when the electron concentration inside a single QW is continuously tuned between $N \approx 0$ and $N = 8\times10^{11}$ cm^{-2}. We report spectroscopic studies of a single $In_{0.53}Ga_{0.47}As$ QW from 10 to 300 K for photon energies varying from below the QW gap to above that of the $In_{0.52}Al_{0.48}As$ barrier material, thus covering the transitions between the $n_z=1$, 2, and 3 subbands. We find that at the $n_z=1$ transition the dominant mechanism is the filling of phase space, whereas at the $n_z=2$ and 3 transitions we observe electrostatic effects causing shifts and broadening of the QW confined states. "Forbidden transitions" become apparent at large electron densities for primarily the same reason as in the quantum-confined Stark effect.[9] All the transitions are assigned by numerical self-consistent calculations of the single-particle eigenstates. At room temperature this assignment is checked by measurement of the total absorption by photocurrent spectroscopy. Finally, from the differential absorption spectra near $n_z=1$ we are able to determine the temperature and concentration of the two-dimensional (2D) electron gas. At room temperature we find good agreement between the value of N determined from optical and from $C(V)$ measurements. Our results demonstrate that optical techniques can provide, *in situ,* direct information on parameters of the 2D electron gas which are important for understanding the physics of field-effect devices.

In order to probe the QW absorption directly through transparent substrate and barrier materials, we have chosen to investigate the lattice-matched InGaAs-QW/InAlAs-barrier system grown on InP substrates. This material system is particularly convenient for optical studies, since it is grown on a large–band-gap substrate (InP), which is transparent at the spectral range where the InGaAs QW absorbs. The continuous control of the electron density in the InGaAs MD QW was performed with an electrode in the same manner as the gate in a field-effect transistor as recently demonstrated.[10] The wafer layer structure is the same as in Ref. 10. It was

grown by molecular-beam epitaxy and the optically active region is an undoped $L_z = 110$-Å InGaAs QW. The unprocessed wafer had a low-field mobility of $\mu = 3.7 \times 10^4$ cm^2/V·s and a sheet carrier density of 1.6×10^{12} cm^{-2}, both determined from Hall measurements at 77 K. Field-effect transistor samples were processed from the wafer[10] with source and drain electrodes and a Schottky gate as shown schematically in Fig. 1(a). The gate-to-source voltage value for which the QW is just empty (pinchoff), $V_\varnothing$, was determined by I-versus-V measurement to be -0.5 V. All of the experiments in this Letter were performed with source and drain at the same potential.

For the optical measurements, the samples were mounted on the cold finger of a cryostat whose temperature could be tuned from 10 to 300 K. The change in transmission of the QW channel, ΔT, was measured as a function of the wavelength as the gate-to-source voltage

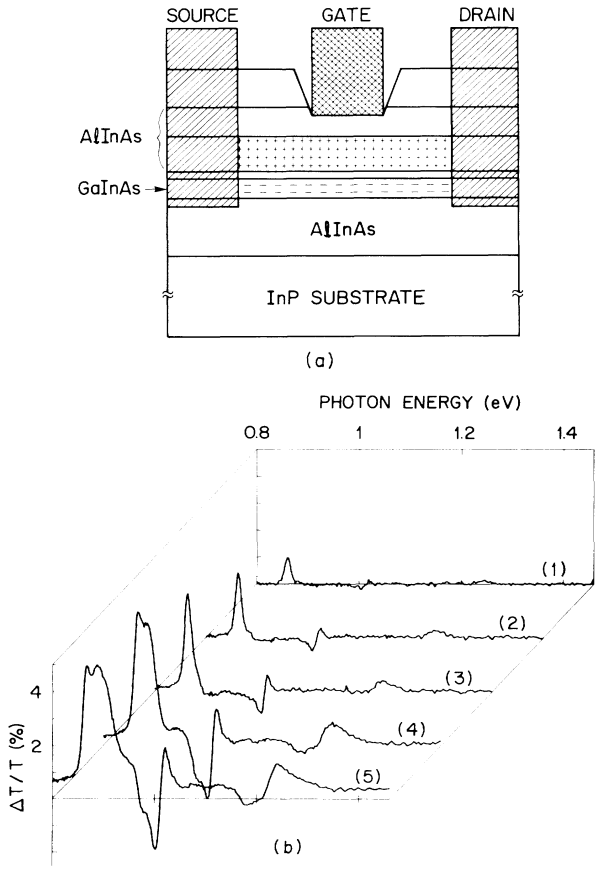

FIG. 1. (a) Structure of field-effect transistor. The 100-Å InGaAs layer is undoped; the InAlAs central layer (250 Å) is doped with Si $\simeq 1.2 \times 10^{18}$ cm^{-3}. (b) Differential absorption spectra, at a lattice temperature of 10 K. Spectra 1 to 5 correspond to gate-source voltage modulation between pinchoff ($V_\varnothing = -0.5$ V) and $V_g = -0.2$, -0.1, 0, $+0.5$, $+1$ V, respectively.

V_g was modulated between $V_\varnothing$ and $V_\varnothing + \Delta V$. For this measurement, a weak light beam was sent from underneath through the transparent substrate and barrier layers, and was detected after reflection off the 100×100-μm^2 Schottky gate. Thus, ΔT is the change in transmission of the probe beam after two passes through the InGaAs QW. In the small-signal regime our experiment determines the differential absorption spectra (DAS): $\Delta T/T \sim (2L_z)\Delta\alpha(\hbar\omega)$, where

$$\Delta\alpha(\hbar\omega) = \alpha^{(0)} - \alpha^{(N)}, \tag{1}$$

and $\alpha^{(0)} = \sum_{n_z} \alpha^{(0)}_{X,n_z} + \alpha^{(0)}_{C,n_z}$ is the absorption coefficient of the empty QW, which comprises the excitonic (X) and continua (C) contributions, and the sum is carried over the heavy-hole (hh) and the light-hole (lh) series. Similarly, $\alpha^{(N)} = \sum_{n_z} \alpha^{(N)}_{X,n_z} + \alpha^{(N)}_{C,n_z}(1 - f_e)$ is the absorption coefficient of the QW containing N electrons. For clarity of the discussion, we distinguish in $\alpha^{(N)}$ the effect of filling of the phase space by the electron distribution f_e, which is described by $1 - f_e$, from the envelope functions $\alpha^{(N)}_{X,n_z}$ and $\alpha^{(N)}_{C,n_z}$ that include all the other changes induced by the 2D electrons.[11,12]

A set of DAS are shown in Fig. 1(b), for $\Delta V = 0.3$–1.5 V. The change of the signal line shape from purely electrostatic effects[9] to carrier-induced effects confirmed accurately the pinchoff value $V_\varnothing = -0.5$ V. We see directly from Eq. (1) that the positive peaks of the DAS correspond to the resonances of the empty QW, where $\alpha^{(0)} > \alpha^{(N)}$, whereas the negative parts come from the spectral regions where $\alpha^{(0)} < \alpha^{(N)}$. These negative parts can originate either because some transitions are shifted or broadened by the introduction of electrons, or because transitions forbidden in the empty QW ($\Delta n_z \neq 0$) become allowed in the presence of electrons. Furthermore, they are readily visible only at high photon energy $\hbar\omega > E_g + E_F$ (E_g and E_F are the gap and Fermi energies, respectively), where the levels are not occupied by electrons ($f_e \ll 1$). Thus, the DAS contain a wealth of information on the electron distribution as well on their effects on the QW energy levels. We demonstrate now how this new spectroscopic tool can be exploited.

First we have checked the assignment of the positive peaks by solving exactly the square-well eigenenergies for the InGaAs/InAlAs system including corrections for the exciton binding energies.[13] An example of the good agreement obtained is shown in Fig. 2, where these transitions are indicated by the top arrows.

Clearly the behaviors close to the $n_z = 1$ transitions and close to the $n_z = 2$ and 3 transitions are very different. At the $n_z = 1$ edge, $\Delta\alpha$ is positive and increases with N until the hh and later the lh exciton peaks appear clearly. This behavior corresponds to the progressive quenching of the absorption as the electrons fill up the bottom of the first conduction subband ($f_e > 0$), up to the point where the total absorption of the empty QW is fully quenched ($f_e \simeq 1$) and $\alpha^{(N)} \approx 0$.[11,12] For the larg-

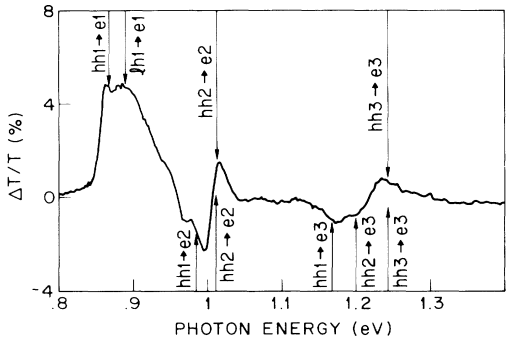

FIG. 2. Position of the energy levels of the empty (top arrows) and full (bottom arrows) QW.

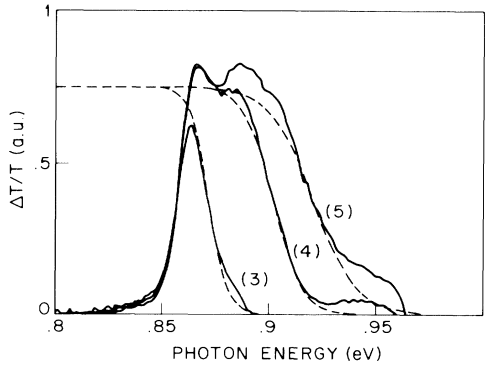

FIG. 3. Detail of the differential spectra line shapes close to the $n_z=1$ transition for the curves 3 to 5 of Fig. 1(b) and Fermi distribution fitted to the high-energy tails. The temperature and concentration determined by the method described in the text are (3) $T_e=50$ K, $N\approx 8\times10^{10}$ cm^{-2}; (4) $T_e=80$ K, $N\approx 4.3\times10^{11}$ cm^{-2}; and (5) $T_e=120$ K, $N\approx 6.4\times10^{11}$ cm^{-2}.

est values of ΔV the height of the hh and lh exciton peaks changes no more ($\Delta T/T\simeq 4\%$, i.e., $\Delta\alpha\simeq 2\times10^4$ cm^{-1}); only the width of the quenched region ($f_e\simeq 1$) continues to increase. At the $n_z=2$ and 3 transitions the signal is smaller with a "differential" line shape showing positive and negative parts indicative of shift and broadening (curves 1, 2, and 3). As ΔV increases, negative low-energy shoulders develop clearly (curves 4 and 5).

In order to understand the origin of these features we have solved the electron and hole Schrödinger and Poisson equations self-consistently in our structure for each V_g [8,14] assuming that the QW contains a density of electrons determined as explained in the next paragraphs. This provides the positions of all the single-particle levels and therefore gives the shifts of the allowed ($\Delta n_z=0$) transitions, as well as the positions of those forbidden in the empty QW that become allowed because of the field generated by the electrons ($\Delta n_z\neq 0$). Both sets of transitions are shown by the bottom arrows in Fig. 2. The shoulders correspond very nicely to the now allowed $\Delta n_z=1$ and 2 hh transitions. The lh transitions shift very little and therefore do not show up in the DAS. The red shift of the $n_z=2$ hh transitions originates from the nonuniform field inside the well (a uniform field would produce a blue shift of this transition). However, as shown in Fig. 2, the magnitude of the calculated shift is too small for shift alone to explain the line shape. A possible additional contribution includes broadening by collisions with the 2D electron gas induced by the electrostatic field in the well. In order to check this interpretation, we have measured directly, at room temperature, the absorption of the empty and of the filled QW using photocurrent spectroscopy. At the $n_z=2$ resonance we observe, indeed, both a shift and a broadening.

It is generally difficult to obtain information on the 2D electron gas inside field-effect transistor structures. Parameters as fundamental as the electron density N are usually evaluated indirectly from modeling of electrical measurements such as $C(V)$. We show now how the line shape of the DAS at $n_z=1$ can be exploited to determine N and the electron temperature T_e. First, we note that the difference between the envelope functions $\alpha^{(0)}_{X,n_z}$ and $\alpha^{(0)}_{C,n_z}$ on one hand, and $\alpha^{(N)}_{X,n_z}$ and $\alpha^{(N)}_{C,n_z}$ on the other, arises from the electrostatic field induced in the QW by the electrons and from many-body effects: BGR and reduction of the exciton binding energy. All these effects modify the position of the gap and the exciton oscillator strength,[11] but they are not very important in the flat continua above the resonances. This is seen from the rather extended regions where $\Delta\alpha(\hbar\omega)\simeq 0$ between the successive resonances on the first three spectra of Fig. 1. Thus fitting of the high-energy tail of the DAS above $n_z=1$ by a Fermi distribution determines accurately the electron temperature T_e as well as the photon energy $\hbar\omega_F=E_{11}(N)+(m_e/m)E_F$, corresponding to N electrons in the conduction band, where E_{11} is the new gap, and m_e,m are the electron and the reduced electron-hole mass.[13] In Fig. 3 we show a set of DAS blown up in this region of the spectrum, together with the fitted Fermi distributions. The two parameters $\hbar\omega_F$ and T_e act almost independently on the position and shape of f_e, thus giving easy and unique fits. We find that $T_e=50$ K as long as the Schottky diode is reverse biased and the leakage current across remains moderate (curves 1 to 3), but T_e increases more quickly when the conditions for forward bias are approached. It reaches 80 and 120 K for the last two curves and can get even higher for very large ΔV. Heating of the lattice is easily ruled out from the position of the front edge of $\Delta\alpha$ which does not change. The heating of the 2D electron gas well above the lattice temperature is in good agreement with the energy-loss rate per carrier in our QW material deduced from the gate-source leakage current.[15]

To relate the electron density in the QW to $\hbar\omega_F$ we need to know the position of the new gap, $E_{11}(N)$

$=E_{11}(0)-\Delta_{ES}-\Delta_{BGR}$. The electrostatic correction Δ_{ES} is readily given by the self-consistent calculation of the shift of the single-particle states. It is much more difficult to account for the many-body effects. Numerical calculations of the correlation-exchange energy in quantum-well structures have shown that the density dependence of the Coulomb-hole potential, which is responsible for most of the BGR at low and moderate density, is well fitted by a $N^{1/3}$ density dependence.[16,17] We have used this functional form to evaluate Δ_{BGR} and hence to calculate N. We have first applied this procedure to the 300-K spectra for which a comparison to $C(V)$ measurements up to $\Delta V=0.5$ V is possible. The agreement is excellent; for example, we find that for $\Delta V=0.5$ V, $N=(3.3\pm0.4)\times10^{11}$ cm^{-2} from the electrical measurements and $N=(3.2\pm0.2)\times10^{11}$ cm^{-2} from our analysis of the DAS. The weak density dependence of the many-body effects, especially when compared to the width of the phase-space filling ($\Delta_{BGR}<8$ meV over the whole range of ΔV), explains why our approximation to account for the BGR suffices. The parameters of the fit for the spectra of Fig. 1 and the corresponding values of N are given in the caption of Fig. 3 and show that large densities are reached.

In conclusion, we have presented a direct investigation of the changes of the absorption spectrum of a single QW caused by the progressive introduction of a 2D electron gas up to large densities. We explain the observed differential absorption spectra by the quenching of the absorption at the fundamental gap, the shift and broadening of the higher transitions, and the appearance of new "forbidden" ones. We have also shown that optical techniques are able to determine the density and temperature of the 2D electron gas in a single QW. Let us note finally that the effects we have observed are large enough to have applications for optoelectroic devices and in optical interconnects for III-V electronics.

[1]For a recent review of semiconductor quantum well physics and application, see the articles in the special issue of IEEE J. Quantum Electron. **22**, No. 9 (1986), edited by D. S. Chemla and A. Pinczuk.

[2]See, for example, R. C. Miller and D. A. Kleinmann, J. Lumin. **30**, 530 (1985); D. S. Chemla, J. Lumin. **30**, 502 (1985).

[3]H. L. Stormer, R. Dingle, A. C. Gossard, W. Wiegmann, and M. D. Sturge, J. Vac. Sci. Technol. **16**, 1517 (1979); H. L. Stormer, Surf. Sci. **132**, 519 (1983).

[4]A. Pinczuk, J. Shah, R. C. Miller, A. C. Gossard, and W. Wiegmann, Solid State Commun. **50**, 735 (1984).

[5]R. Sooryakumar, D. S. Chemla, A. Pinczuk, A. C. Gossard, W. Wiegmann, and L. J. Sham, Solid State Commun. **54**, 859 (1985).

[6]A. E. Ruckenstein, S. Schmitt-Rink, and R. C. Miller, Phys. Rev. Lett. **56**, 504 (1986).

[7]M. H. Meynadier, J. Orgonasi, J. A. Brum, G. Bastard, M. Voos, G. Weimann, and W. Schlapp, Phys. Rev. B **34**, 2482 (1986).

[8]C. Delalande, J. Orgonasi, M. H. Meynadier, J. A. Brum, G. Bastard, G. Weimann, and W. Schlapp, Solid State Commun. **59**, 613 (1986).

[9]D. A. B. Miller, D. S. Chemla, T. C. Damen, A. C. Gossard, W. Wiegmann, T. H. Wood, and C. A. Burrus, Phys. Rev. B **32**, 1043 (1985); D. A. B. Miller, J. S. Weiner, and D. S. Chemla, IEEE J. Quantum Electron. **22**, 1816 (1986).

[10]D. S. Chemla, I. Bar-Joseph, C. Klingshirn, D. A. B. Miller, J. M. Kuo, and T. Y. Chang, Appl. Phys. Lett. **50**, 585 (1987).

[11]S. Schmitt-Rink, D. S. Chemla, and D. A. B. Miller, Phys. Rev. B **32**, 6601 (1985).

[12]D. A. Kleinmann, Phys. Rev. B **32**, 3766 (1985).

[13]J. S. Weiner, D. S. Chemla, D. A. B. Miller, T. H. Wood, D. Sivco, and A. Y. Cho, Appl. Phys. Lett. **46**, 619 (1985).

[14]G. Livescu, I. Bar-Joseph, D. A. Miller, and D. S. Chemla, unpublished.

[15]J. Shah, IEEE J. Quantum Electron. **22**, 1728 (1986).

[16]S. Schmitt-Rink and C. Ell, J. Lumin. **30**, 585 (1985).

[17]D. A. Kleinmann and R. C. Miller, Phys. Rev. B **32**, 2266 (1985).